ISSN 1330-3651 (Print), ISSN 1848-6339 (Online)
https://doi.org/10.17559/TV-20230308000422
Preliminary communication

# The Influence of Material Storage on Mechanical Properties and Deterioration of Composite Materials

Sara RADOJIČIĆ*, Pejo KONJATIĆ, Marko KATINIĆ, Josip KAČMARČIK

**Abstract:** This article focused on the experimental and statistical analysis of the mechanical properties of dog-bone samples manufactured by fused deposition modelling (FDM). Two identical materials were examined, i.e., Onyx with carbon fiber but from different series and differently stored. One was kept in the manufacturer package and the other one was kept in machine storage box. The paper explains how the samples with various numbers of fiber layers and printing infill were created, 3D printed, measured to evaluate their accuracy in dimensions, exposed to tensile test, and reviewed. At this stage of investigation, the paper is limited to static tests of materials. The data presented here will be of great assistance for additional studies intended for the filament deposition development and modification of the basic material through the combinations with different composites, such as carbon fiber. It was discovered with this research that the mechanical properties of test samples created by FDM can differ based on the manufacturer series. This issue has not been studied thoroughly, so far. Research, by analysing the key variable, which is the batch of 3D print material, offers important new data to engineers and designers. It also prepares the ground for advanced studies and research in respect of the weakness and strength analysis of the 3D printed models.That is very relevant for the optimizing structures in this modern age and the industrial era 4.0 as well as the development in the LEAN process of manufacturing.

**Keywords:** additive manufacturing; carbon fiber; composite materials; continuous fiber fabrication; tensile test

## 1 INTRODUCTION

The modern life without unreinforced polymers and fibre reinforced polymers is hard to imagine. Today, it is an essential part of people's lifestyle, with products that range from consumer products to complex scientific products. Without these multipurpose and cost-effective materials, numerous technical miracles would not be possible [1].

The process of fabrication of CFRP composites has been transformed with the progress of additive manufacturing technology. It stands for Continuous Fiber Reinforced Polymer composites and finished products have specific structure and material, making them very complex [2]. Process used to additively manufacture fibre composites is Fused Deposition Modelling process (FDM) [3-5]. This process was developed by the company called MarkForged, and it requires the deposition of fibre-thermoplastic filaments layer-by-layer where a hot extrusion process is used to construct the composite material. It has been used to 3D print parts that are reinforced with continuous fibres of carbon [6-9], glass [10-12], aramid [13, 14] and jute [15, 16].

3D printer filament can expire and its mechanical properties can detoriate over time just like any other item that has a shelf life. With 3D printer filament, the storage environment is very important. It must be stored in moisture-free conditions to last, and its shelf life is significantly affected by the presence of humid conditions that contain moisture. To avoid moisture, filament manufacturers provide instructions for storing their filament under very specific conditions. This protects the filament from damage. The list of problems resulting from exposure to moisture is long and is based on the filament's absorption of moisture through the air. The outer part of the filament can become brittle after being exposed to moisture or humid conditions, and the quality of prints made with the filament will no longer be optimal, but this is easily overlooked. If the filament is constantly exposed to moisture and humid environments, this can lead to increased brittleness, degradation of the filament, larger diameter and filament breakage [17-20].

The influence of material age on the mechanical properties of 3D printed fiber-reinforced continuous polymers was investigated in this paper. Specimens with different infill percentage and different numbers of layers were fabricated and analyzed. To the best of our knowledge, the relevant time deterioration research of 3D printed fiber-reinforced composites is extremely limited. The relationship between the numbers of layers, infill percentage and mechanical properties of these materials was discussed in detail. In combination with the different batch series of the same 3D printer filament, a comprehensive statistical analysis of the given mechanical properties of these composites was made.

## 2 MATERIALS

The FDM filament studied is polyamide enriched with carbon fibers. It represents a representative sample of thermoplastic material used for 3D printing of composites. The filament used is called Onyx, and the reinforcement used for both sets of samples is Carbon Fiber by MarkForged. Onyx is a filament that represents two fused materials, nylon and carbon fibers. The stiffness of 3D printed part is increased due to the chopped fibers of carbon fiber. It provides reinforcement that will improve stiffness, strength, and dimension accuracy. Carbon Fiber is MarkForged's Continuous Fiber and it has very high strength and stiffness. Parts can be as strong as 6061-T6 Aluminum when Carbon fiber is placed in a Base material such as Onyx.

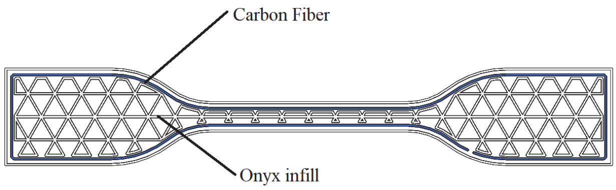


**Figure 1** The cross-section of the test sample

The cross-section of the test sample that is shown in Fig. 1 is a sample that was printed in the combination of 6 fibre layers and 41% infill. Materials used for this combination are Carbon Fibre for the fibre material and Onyx for the infill material. Fig. 1 represents the 7th layer of the sample cross section where the fiber is shown in blue and the Onyx infill in white.

The carbon fibers are distributed evenly in the sample, and one of the factors in the experimental plan was the filling density, which was varied with 28%, 41% and 54%. Additionally, the number of reinforcement layers is varied to 4, 6 and 8 layers. Two sets of samples were printed. One was printed with material that had been in the printer's chamber for approximately 18 months, while the second set of samples was printed with new material from a different batch, but from the same manufacturer, so that the results could be compared. This material was stored in a special Drybox, shown in Fig. 2, that protects the filament from moisture and ensures dryness. That will lead to the best possible performance and better overall results.

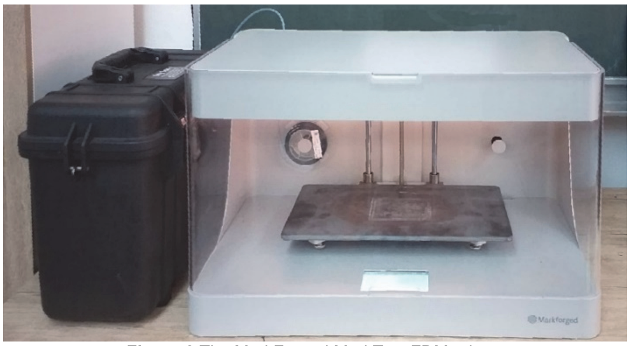

**Figure 2** The MarkForged MarkTwo FDM printer

## 3 EXPERIMENTAL SETUP

### 3.1 Test Gearbox and Instrumentation

A MarkForged MarkTwo FDM printer, shown in Fig. 2, was used for 3D printing and it has one print head. Inside, that print head contains two nozzles that are separate from each other. One nozzle is used to print polymer material, while the other is used to print fiber-polymer material. The print head can operate one nozzle at time so the interaction and contact between the fiber-polymer filament and the polymer filament does not exist. In order to print a basic block of the 3D printed part, all stages of the FDM process must be performed continuously. Approach for this process is layer-by-layer approach. Software used for 3D printing is the Eiger software and it is the official slicer used by all Markforged printers. The 3D setup of the sample is shown in Fig. 3.

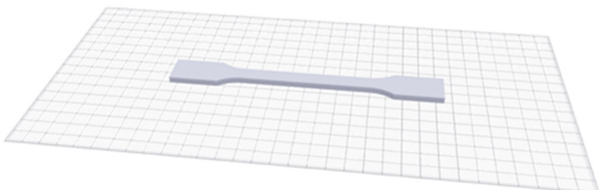

**Figure 3** The 3D setup of the test sample

The MarkForged Mark Two uses CFR additive manufacturing process which is Continuous Fiber Reinforcement process. It is an augmented FFF (Fused Filament Fabrication) used to lay enrich the printed part with continuous fibers. As already stated, it has two separate nozzles where the second nozzle is used to print strands of special fibers inside a conventional polymer part. Fibers used for reinforcement of the 3D printed parts increase overall stiffness and strength. This way, parts 3D printed with CFR can achieve metal-strength properties while being lightweight.

The printer uses both nozzles for printing, first it makes the base thermoplastic material and after it lays down layers of continuous fibers on the part. Formation of one layer has two steps. First, an extrusion of a thermoplastic will occur and it will be the "matrix" of that composite. Second, the continuous fiber will be fused with the polymer and ironed into matrix. The explained process is repeated layer by layer. It is important to mention that not every layer is reinforced with fibers and these steps describe printing of fiber reinforced layers. In order to optimize ratio of part's weight and strength, continuous fibers can be made into special patterns.The fiber can also be placed in specific areas of the 3D printed part based on the external load.

**Table 1** Mechanical and physical properties of used materials

| Properties | Material | |
|---|---|---|
| | Onyx | Carbon Fiber |
| Density / g/cm$^3$ | 1,2 | 1,4 |
| Tensile Modulus / GPa | 2,4 | 60 |
| Flexural Strength/ MPa | 71 | 540 |
| Tensile Strain at Break / % | 25 | 1,5 |
| Flexural Modulus / GPa | 3 | 51 |

### 3.2 Tensile Test

As part of the work, a static tensile test was performed for two different sets of data. During the static tensile test, data were obtained on the mechanical properties of individual materials at room temperature. The experimental plan is shown in the Tab. 2. Every test sample consists of 16 layers each having the same layer height of 0,125 mm. That is a height measure of each following addition of material. The total height of the sample is 2 mm. Of the total number of layers, only a part is reinforced with Carbon Fiber. Number of reinforced layers for each test sample is given in Tab. 2, as well as the density percentage of Onyx. Maximum number of fiber reinforced layers that was possible in the Eiger software is 8.

**Table 2** Plan of experiment

| Number | Density / % | Number of CF layers |
|---|---|---|
| 1 | 28 | 4 |
| 2 | 54 | 4 |
| 3 | 28 | 8 |
| 4 | 54 | 8 |
| 5 | 28 | 6 |
| 6 | 54 | 6 |
| 7 | 41 | 4 |
| 8 | 41 | 8 |
| 9 | 41 | 6 |
| 10 | 41 | 6 |
| 11 | 41 | 6 |
| 12 | 28 | 0 |
| 13 | 41 | 0 |
| 14 | 54 | 0 |

The test parameters of materials are regulated by the ISO 527-1 standard for tests at room temperature. The procedure is suitable for materials: rigid and semi-rigid plastomer, but excluding fibers (ISO 527-4 and ISO 527-5), duromers and thermotropic liquid crystal polymer. The test was performed on sample 5A selected according to the previously mentioned norm. The dimensions of the sample are shown in Fig. 4 and dimensions in Tab. 3.

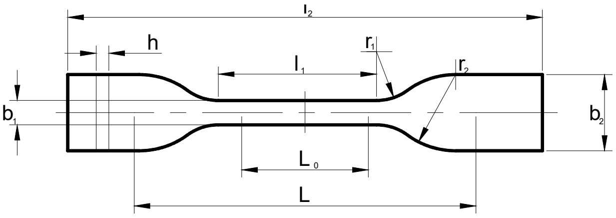


**Figure 4** The dimensions of the test sample

**Table 3** Dimensions of 5A test sample

| | Dimensions / mm |
|---|---|
| Sample type | 5A |
| $l_2$ | ≥ 75 |
| $b_2$ | 12,5 ± 1 |
| $l_1$ | 25 ± 1 |
| $b_1$ | 4 ± 0,1 |
| $r_1$ | 8 ± 0,5 |
| $r_2$ | 12,5 ± 1 |
| $L$ | 50 ± 2 |
| $L_0$ | 20 ± 0,5 |
| $h$ | ≥ 2 |

The test samples were tested at room temperature at a speed of 2 mm/min on an Instron tensile testing machine. Based on the results obtained from the testing machine, an analysis was made. The dimensions of all samples were controlled, measured in three places and the arithmetic mean was taken in order to obtain a more accurate cross-sectional area, since deviations from the intended dimensions occur during printing. The values obtained as a result were used to calculate the maximum stress, modulus of elasticity and deformation.

## 4 EXPERIMENTAL RESULT AND DISCUSSION

The experiment was conducted in such a way that two sets of samples were printed: old (sat in the printer for a period of 18 months) and new sample of the same type of material. 3D test samples are printed in 14 combinations considering number of layers (0, 4, 6 and 8 layers) and the percentage of infill (28%, 41% and 54% of infill). In the combination of 6 layers and 41% infill, 3 test samples were printed, while for the others only one test sample was printed in each of the two material sets. In further analysis, in order to ensure the independence of the samples, as representatives of the maximum stress, in the combination of 6 layers and 41% infill, the average of three measured values was used. Fig. 5 shows a test sample after the static tensile test.

**Figure 5** The test sample after the static tensile test

Both sets of samples were tested in the same way. First, samples of the old material that had been in the 3D printer for a year were tested on the tensile test machine, and then samples of new material from a different batch that was packaged by the manufacturer MarkForged were tested. As can be seen in Fig. 6 and Fig. 7, every test sample was marked to avoid mistakes when calculating the values for maximum stress, modulus of elasticity and deformation.

**Figure 6** The test sample after the static tensile test

**Figure 7** The test sample after the static tensile test

Using the data obtained from the static tensile test machine, the values for maximum stress, modulus of elasticity and deformation were calculated, and the obtained results are shown in the Tab. 4. The letters O and N represent old or new, depending on whether it is an old or a new sample set.

**Table 4** Results of the static tensile test

| Number | Maximum Stress / MPa | Deformation | Modulus of Elasticity / MPa |
|---|---|---|---|
| O 1 | 95,63 | 0,05 | 2426,90 |
| O 2 | 92,14 | 0,05 | 2424,82 |
| O 3 | 136,44 | 0,06 | 3287,35 |
| O 4 | 128,07 | 0,06 | 3285,56 |
| O 5 | 109,55 | 0,05 | 2925,74 |
| O 6 | 123,39 | 0,06 | 2787,36 |
| O 7 | 100,18 | 0,06 | 2300,99 |
| O 8 | 139,35 | 0,07 | 3216,57 |
| O 9 | 117,65 | 0,06 | 2909,60 |
| O 10 | 117,15 | 0,06 | 2847,78 |
| O 11 | 120,31 | 0,06 | 2768,24 |
| O 12 | 36,64 | 0,37 | 695,62 |
| O 13 | 36,06 | 0,40 | 694,89 |
| O 14 | 35,66 | 0,41 | 652,14 |
| N 1 | 97,29 | 0,06 | 2287,73 |
| N 2 | 94,00 | 0,06 | 2172,84 |
| N 3 | 127,62 | 0,07 | 2944,62 |
| N 4 | 131,29 | 0,06 | 3086,33 |
| N 5 | 103,32 | 0,05 | 2693,78 |
| N 6 | 110,52 | 0,07 | 2637,36 |
| N 7 | 90,56 | 0,06 | 2129,91 |
| N 8 | 121,56 | 0,07 | 2815,49 |
| N 9 | 108,85 | 0,07 | 2399,93 |
| N 10 | 102,21 | 0,06 | 2539,65 |
| N 11 | 105,04 | 0,06 | 2539,59 |
| N 12 | 32,76 | 0,36 | 592,07 |
| N 13 | 32,48 | 0,37 | 581,05 |
| N 14 | 31,65 | 0,37 | 541,61 |

Considering the obtained results, the values of the differences in test results of samples from old and new material were calculated for each of the obtained values. These percentages are shown in Tab. 5.

**Table 5** Differences in test results of samples from old and new material

| Number | (Old – New) / New | | |
|---|---|---|---|
| | Maximum Stress / MPa | Deformation | Modulus of Elasticity / MPa |
| 1 | −1,7% | −16,7% | 6,1% |
| 2 | −2,0% | −16,7% | 11,6% |
| 3 | 6,9% | −14,3% | 11,6% |
| 4 | −2,5% | 0,0% | 6,5% |
| 5 | 6,0% | 0,0% | 8,6% |
| 6 | 11,6% | −14,3% | 5,7% |
| 7 | 10,6% | 0,0% | 8,0% |
| 8 | 14,6% | 0,0% | 14,2% |
| 9 | 8,1% | −14,3% | 21,2% |
| 10 | 14,6% | 0,0% | 12,1% |
| 11 | 14,5% | 0,0% | 9,0% |
| 12 | 11,8% | 2,8% | 17,5% |
| 13 | 11,0% | 8,1% | 19,6% |
| 14 | 12,7% | 10,8% | 20,4% |
| Average | 8,3% | −3,9% | 12,3% |

Analyzing the differences results, it is clearly visible that the old set of samples has higher values of maximum stress and modulus of elasticity, and lower values of deformation. Results are significantly lower than the data given by the manufacturer. That is becase the infill of 3D print is not 100% and evey combination of printing infill and number of reinforced layers is different and created a unique combination. Above described differences in test results are also shown in Fig. 8.

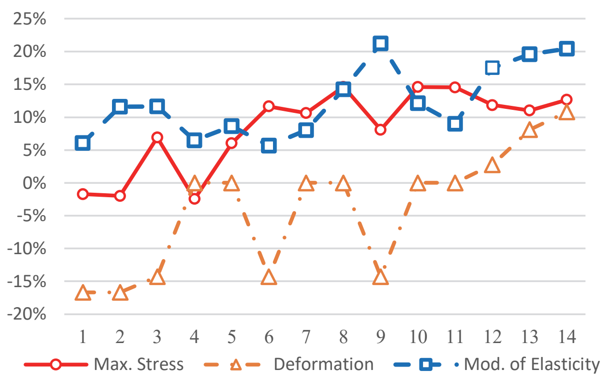


**Figure 8** Differences in test results of samples from old and new material

## 4.1 Maximum Stress

The goal of the analysis is to determine whether there is a significant effect of the age of the used material on the maximum stress of the same, measured in MPa. In the analysis, the *t*-test for paired samples (the justification of which is commented below) was used, whereby the pairing is done considering the combination of the number of layers and the percentage of infill. The graphic representation of all the data of the maximum stress by the number of layers and percentage of infill is shown on Fig. 9. The Shapiro-Wilk test is a test of normality and it is used to check the normality of the distribution of the data set. It is used on sets of 3 to 50 elements. The Shapiro-Wilk test does not reject the assumption of normality of the differences in the maximum stress for the paired samples considering the combination of the number of layers and the percentage of filling ($W$ = 0,95632; $p$-value = 0,7320). The $F$-test does not reject the assumption of homoscedasticity (equality of variance with respect to the age of the material; $F$ = 1,1171; $p$-value = 0,8146).

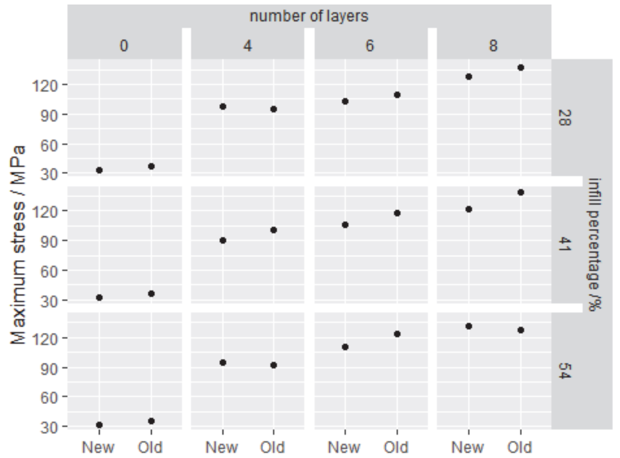


**Figure 9** The graphic representation of all the data of the maximum stress by the number of layers and percentage of infill

Fig. 10 represents the boxplot diagram of the maximum stress with respect to the age of the material.

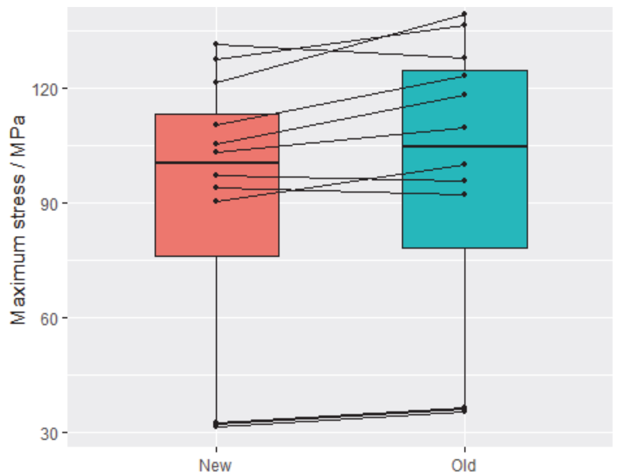


**Figure 10** The boxplot diagram of the maximum stress with respect to the age of the material

There is a statistically significant difference in the maximum stress of the printed test samples, considering the age of the material ($p$-value = 0,008368 < 0,05; $t$ = 3,2058). The average value of the difference in maximum stress between the test samples printed with the old and the new material is 6,089256, with a 95% confidence interval (1,908557; 10,269954). Therefore, the expected maximum stress of test samples printed with old material is higher than the same for test samples printed with new material.

## 4.2 Modulus of Elasticity

The *t*-test for paired samples was also used for the analysis of the age of the used material and its impact on the modulus of elasticity of the same, measured in MPa. The pairing in the above mentioned test is done considering the combination of the number of layers and the percentage of infill. As for the modulus of elasticity, the graphic representation of all the data is shown in Fig. 11.

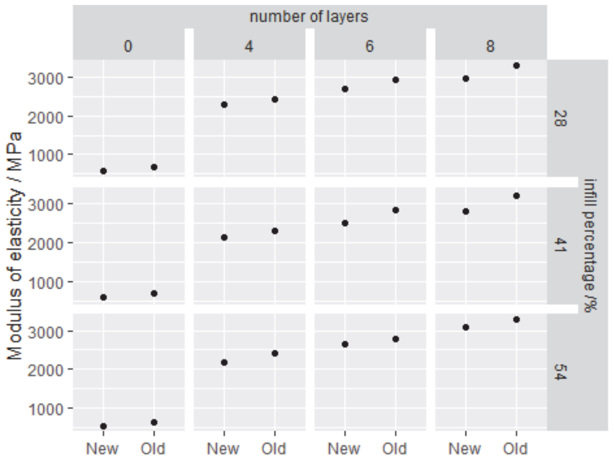

**Figure 11** The graphic representation of all the data of the Modulus of Elasticity by the number of layers and percentage of infill

Results of the Shapiro-Wilk test for the modulus of elasticity are similar to the results of the same test for the Maximum Stress as it does not reject the assumption of normality of the differences for the paired samples considering the same combination of the number of layers and the percentage of infill ($p$-value = 0,1295; $W$ = 0,89317). The assumption of homoscedasticity is not rejected by the $F$-test (equality of variance with respect to the age of the material; $F$ = 1,1559; $p$-value = 0,8144). The boxplot diagram of the modulus of elasticity with respect to the age of the material is shown in Fig. 12.

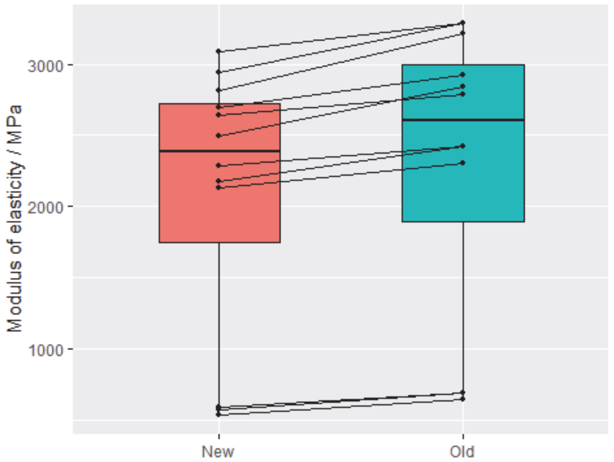

**Figure 12** The boxplot diagram of the Modulus of Elasticity with respect to the age of the material

There is a statistically significant difference in the modulus of elasticity of the printed samples, considering the age of the material ($p$-value = $1,749\times e^{-5} < 0,05$; $t$ = 7,2015). The average value of the difference in modulus of elasticity between the test samples printed with the old and the new pattern is 213,6644 MPa, with a 95% confidence interval (148,3626 Mpa; 278,9661 MPa). Therefore, the expected modulus of elasticity of test samples printed with old material is higher than the same for test tubes printed with new material.

### 4.3 Deformation

For the last part of the statistical analyisis, the goal is to determine whether the significant effect of the age of the used material on the percentage of its deformation exists. Fig. 13 represents all the data of the deformation.

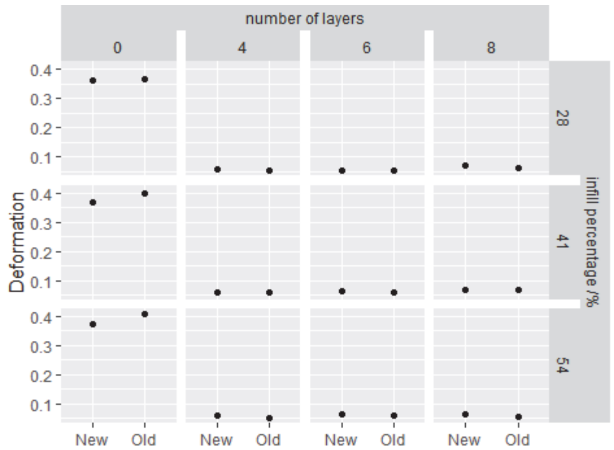

**Figure 13** The graphic representation of all the data of the deformation by the number of layers and percentage of infill

Unlike the test results for the maximum stress and the modulus of elasticity, The Shapiro-Wilk test rejects the assumption of normality of the differences in the deformation for the samples paired considering the combination of the number of layers and the percentage of infill ($W$ = 0,75136; $p$-value = 0,002761 < 0,05). Therefore, in the analysis, the Wilcoxon test for paired samples was used and it is the non-parametric equivalent of the t-test for paired samples. The pairing is done considering the combination of the number of layers and the percentage of infill and the boxplot diagram of the deformation with respect to the age of the material is shown in Fig. 14.

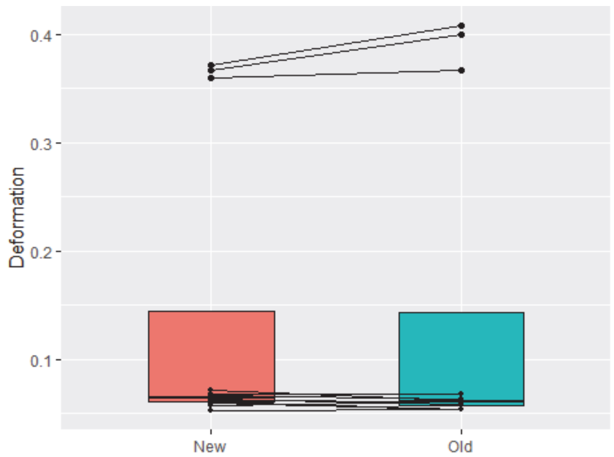

**Figure 14** The boxplot diagram of the Deformation with respect to the age of the material

Using the Wilcoxon test, there was no statistically significant difference in the percentage of deformation of the printed test samples, considering the age of the material ($V$ = 38, $p$-value = 0,9697).

## 5 CONCLUSIONS

In this paper, specimens with different print infill percentage and number of carbon fiber layers were printed. One set was printed with the material that was in the 3D printer for 18 months and the other with the material that was new and sealed, both from the same manufacturer. In addition, both sets of test samples were tested and examined on the static tensile testing machine. The results of the statistical analysis, performed considering the combination of the number of layers and the percentage of infill showed that there is a significant difference in the maximum stress and the modulus of elasticity of the printed test samples. Somewhat unexpectedly, the old material showed a higher modulus of elasticity and strength but the differences are still not substantial, considering all the uncertainties that can affect the final result (filament production, printing process, tensile test). However, there was no statistically significant difference in the percentage of deformation of the printed test specimens when the age of the material was taken into account.

There are several explanations for these differences, one of which is different batches of the same material. Even if it is the same material, each batch is unique and there will always be variations in mechanical properties. Second, the storage of these materials may be in question if the old material that was in the printer for a year was stored in a hermetically sealed room inside the 3D printer and the new material was stored in the manufacturer's box. MarkForgedDrybox is obviously a very good tool for storing filament. Research has shown that after 18 months, no signs of material degradation can be observed. Thus, the Drybox enables storage in similar conditions as in the original packaging of the material. The humidity of the room is also an issue that needs further investigation and can be a major problem for printing even though this research did not prove an impact. However, 18 months is not a sufficient period for the appearance of degradation effects due to humidity. Also, the new material is the same age as the old, only it was in the factory packaging and unopened. All of these reasons are influential and this work will contribute to the application of 3D printed composites. This research addresses potential problems in storage and use of composites and will be useful for any direction of future research.

## 6 REFERENCES

[1] Navaratnam, S., Selvaranjan, K., Jayasooriya, D., Rajeev, P., & Sanjaan, J. (2017). Applications of natural and synthetic fiber reinforced polymer in infrastructure: A suitability assessment. *Journal of Building Engineering*, *66*, 10583. https://doi.org/10.1016/j.jobe.2023.105835

[2] Parandoush, P. & Lin, D. (2017). A review on additive manufacturing of polymer-fiber composites. *Composite Structures*, *182*, 36-53. https://doi.org/10.1016/j.compstruct.2017.08.088

[3] Ismail, K. I., Yap, T. C., & Ahmed, R. (2022). 3D-Printed Fiber-Reinforced Polymer Composites by Fused Deposition Modelling (FDM): Fiber Length and Fiber Implementation Techniques. *Polymers*, *14*, 4659. https://doi.org/10.3390/polym14214659

[4] Turner, B. N., Strong, R., & Gold, S. A. (2014). A Review of Melt Extrusion Additive Manufacturing Processes: I. Process Design and Modeling. *Rapid Prototyping Journal*, *20*, 192-204. https://doi.org/10.1108/RPJ-01-2013-0012

[5] Chacón, J. M., Caminero, M. A., García-Plaza, E., & Núñez, P. J. (2017). Additive manufacturing of PLA structures using fused deposition modelling: Effect of process parameters on mechanical properties and their optimal selection. *Materials &Design*, *124*, 143-157. https://doi.org/10.1016/j.matdes.2017.03.065

[6] Galos, J., Hu, Y., Radvindran, A. R., Ladani, R. B., & Mouritz A. P. (2021). Electrical properties of 3D printed continuous carbon fibre composites made using the FDM process.*Composites Part A: Applied Science and Manufacturing*, *151*, 1106661. https://doi.org/10.1016/j.compositesa.2021.106661

[7] Giani, N., Mazzocchetti, L., Benelli, T., Picchioni, F., & Giorgini, L. (2022). Towards sustainability in 3D printing of thermoplastic composites: Evaluation of recycled carbon fibers as reinforcing agent for FDM filament production and 3D printing.*Composites Part A: Applied Science and Manufacturing*, *159*, 107002. https://doi.org/10.1016/j.compositesa.2022.107002

[8] Hu, Y., Ladani, R. B., Brandt, M., Li, Y., & Mouritz, A. P. (2021). Carbon fibre damage during 3D printing of polymer matrix laminates using the FDM process. *Materials & Design*, *205*, 109679. https://doi.org/10.1016/j.compositesa.2022.107002

[9] Demir, I., Sevim, O., Ogdu, M. K., Dogan, O., & Demir, S. (2021). Mechanical and Physical Properties of Autoclaved Aerated Concrete Reinforced Using Carbon Fibre of Different Lengths. *Tehnički vjesnik*, *28*(2), 503-508. https://doi.org/10.17559/TV-20200218194755

[10] Cao, L., Xiao, J., Kim, J. K., & Zhang, X. (2023). Effect of post-process treatments on mechanical properties and surface characteristics of 3D printed short glass fiber reinforced PLA/TPU using the FDM process. *CIRP Journal of Manufacturing Science and Technology*, *41*, 135-143. https://doi.org/10.1016/j.cirpj.2022.12.008

[11] Štefić, T., Jurić, A., & Marović, P. (2011) Determination of modulus of elasticity for glass fibre reinforced polymers. *Tehnički vjesnik*, *18*(1), 69-72.

[12] Sodeifian, G., Ghaseminejad, S., & Yousefi, A. A. (2019). Preparation of polypropylene/short glass fiber composite as Fused Deposition Modeling (FDM) filament. *Results in Physics*, *12*, 205-222. https://doi.org/10.1016/j.rinp.2018.11.065

[13] Nagendra, J., Srinath, M. K., Bopanna, K. D., Sujeeth Swamy, S., & Ravikumar, M. (2023). Process parameter optimisation of fused deposition modelling for augmenting the strength of nylon-aramid PMC's. *Materials Today: Proceedings*. https://doi.org/10.1016/j.matpr.2023.01.090

[14] Nagendra, J., Srinath, M. K., Sujeeth, S. S., Naresh, K. S., & Ganesha, P. M. S. (2021). Optimization of process parameters and evaluation of surface roughness for 3D printed nylon-aramid composite. *Materials Today: Proceedings*, *44*, 674-682. https://doi.org/10.1016/j.matpr.2020.10.609

[15] Sola, A. & Trinchi, A. (2023). Chapter 8 - Fused deposition modeling of polymer-matrix composites with natural fibers. *In Woodhead Publishing Series in Composites Science and Engineering, Fused Deposition Modeling of Composite Materials*, 189-210. https://doi.org/10.1016/B978-0-323-98823-0.00005-6

[16] Deb, D. & Jafferson, J. M. (2021). Natural fibers reinforced FDM 3D printing filaments. *Materials Today: Proceedings*, *46*, 1308-1318. https://doi.org/10.1016/j.matpr.2021.02.397

[17] Dzul-Cervantes, M. A. A, Pacheco-Salazar, O. F., Can-Herrera, L. A., Moreno-Chulim, M. V., Cauich-Cupul, J. I., Herrera-Franco, P. J., & Valadez-González, A. (2020). Effect of moisture content and carbon fiber surface treatments on the interfacial shear strength of a thermoplastic-modified epoxy resin composites. *Journal of Materials Research and Technology*, *9*, 15739-15749. https://doi.org/10.1016/j.jmrt.2020.11.027

[18] Petrény, R. & Mészáros, L. (2022). Moisture dependent tensile and creep behaviour of multi-wall carbon nanotube and carbon fibre reinforced, injection moulded polyamide 6 matrix multi-scale composites. *Journal of Materials Research and Technology*, *16*689-699. https://doi.org/10.1016/j.jmrt.2021.12.030

[19] Krstulović-Opara, L., Klarin, B., Neves, P., & Domazet, Ž. (2011). Thermal imaging and Thermal Stress Analysis of the impact damage of composite materials. *Engineering failure analysis*, *18*, 713-719. https://doi.org/10.1016/j.jmrt.2021.12.030

[20] Vizentin, G. & Vukelić, G. (2020). Degradation and damage of composite materials in marine environment. *Materials Science-Medziagotyra*, *26*, 337-342. https://doi.org/10.1016/j.jmrt.2021.12.030

**Contact information:**

**Sara RADOJIČIĆ**, PhD Student
(Corresponding author)
University of Slavonski Brod,
Mechanical Engineering Faculty in Slavonski Brod,
Trg Ivane Brlić Mažuranić 2, HR-35000 Slavonski Brod, Croatia
E-mail: sradojicic@unisb.hr

**Pejo KONJATIĆ**, Prof.
University of Slavonski Brod,
Mechanical Engineering Faculty in Slavonski Brod,
Trg Ivane Brlić Mažuranić 2, HR-35000 Slavonski Brod, Croatia
E-mail: pkonjatic@unisb.hr

**Marko KATINIĆ**, Prof.
University of SlavonskiBrod,
Mechanical Engineering Faculty in Slavonski Brod,
Trg Ivane Brlić Mažuranić 2, HR-35000 Slavonski Brod, Croatia
E-mail: mkatinic@unisb.hr

**Josip KAČMARČIK,** Prof.
University of Zenica,
Faculty of Mechanical Engineering in Zenica,
Fakultetska 1, BiH-72000 Zenica, Bosnia and Herzegovina
E-mail: josip.kacmarcik@unze.ba